

A room-temperature TiO₂-nanotube hydrogen sensor able to self-clean photoactively from environmental contamination

Gopal K. Mor

*Department of Electrical Engineering and Department of Materials Science and Engineering,
217 Materials Research Laboratory, The Pennsylvania State University,
University Park, Pennsylvania 16802*

Maria A. Carvalho

Department of Chemical Engineering, 267 Materials Research Laboratory, The Pennsylvania State University, University Park, Pennsylvania 16802

Ooman K. Varghese

*Department of Electrical Engineering and Department of Materials Science and Engineering,
217 Materials Research Laboratory, The Pennsylvania State University,
University Park, Pennsylvania 16802*

Michael V. Pishko

Department of Chemical Engineering, 267 Materials Research Laboratory, The Pennsylvania State University, University Park, Pennsylvania 16802

Craig A. Grimes

*Department of Electrical Engineering and Department of Materials Science and Engineering,
217 Materials Research Laboratory, The Pennsylvania State University,
University Park, Pennsylvania 16802*

(Received 14 August 2003; accepted 13 November 2003)

Described is a room-temperature hydrogen sensor comprised of a TiO₂-nanotube array able to recover substantially from sensor poisoning through ultraviolet (UV) photocatalytic oxidation of the contaminating agent; in this case, various grades of motor oil. The TiO₂ nanotubes comprising the sensor are a mixture of both anatase and rutile phases, having nominal dimensions of 22-nm inner diameter, 13.5-nm wall thickness, and 400-nm length, coated with a 10-nm-thick noncontinuous palladium layer. At 24 °C, in response to 1000 ppm of hydrogen, the sensors show a fully reversible change in electrical resistance of approximately 175,000%. Cyclic voltammograms using a 1 N KOH electrolyte under 170 mW/cm² UV illumination show, for both a clean and an oil-contaminated sensor, anodic current densities of approximately 28 mA/cm² at 2.5 V. The open circuit oxidation potential shows a shift from 0.5 V to -0.97 V upon UV illumination.

I. INTRODUCTION

A critical concern of any sensor platform is the potential for unwanted contamination, or poisoning, which introduces spurious measurements and generally ends the useful lifetime of a sensor. A sensor used in a noncontrolled environment faces potential contamination from volatile organic vapors, carbon soot, oil vapors, as well as dust and pollen to name but a few examples. An important advance in sensor technology would be a sensor able to self-clean, thereby extending its useful lifetime

and minimizing the potential for spurious measurements. Our motivation is to develop chemical sensors of high performance that are low cost, mechanically robust, and able to self-clean thereby significantly extending their useful lifetime. TiO₂ is well known for its utility as a gas sensor,¹⁻⁵ and its ability to degrade photocatalytically a wide range of substances including organic materials,^{6,7} pesticides,⁸⁻¹² and herbicides.¹³⁻¹⁸

In this work, we use sensors composed of TiO₂ nanotube arrays (Fig. 1) made by an anodization technique.¹⁹ TiO₂ is an *n*-type semiconductor; with ultraviolet photon absorption, an electron-hole pair is generated that can facilitate reduction and oxidation chemistry at the surface of the material. These redox reactions clean the surface

^{a)}Address all correspondence to this author.
e-mail: cgrimes@enr.psu.edu

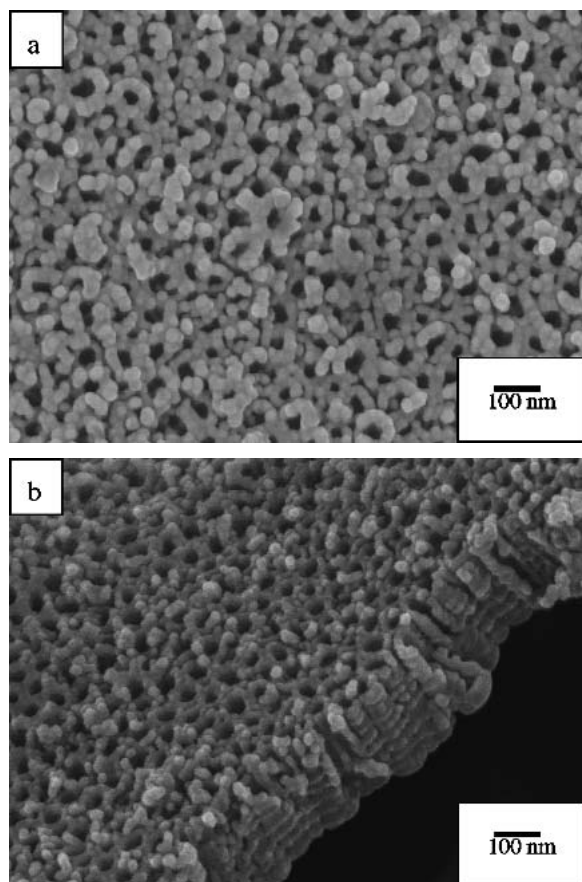


FIG. 1. FE-SEM images of the nanotube array prepared using an anodization potential of 10 V: (a) top view, and (b) cross-sectional view.

by breaking down organic contaminants to form mainly CO₂ and H₂O.²⁰ TiO₂ films also demonstrate the ability to switch from hydrophobic to hydrophilic surfaces after irradiation with UV light,^{21,22} which, together with its photocatalytic properties, has resulted in demonstrating antifogging and self-cleaning capabilities. TiO₂ films are used as the active layer on the recently commercialized self-cleaning windows^{23,24} and are known for their photocatalytic oxidation of contaminants in air.^{25,26}

Factors improving photocatalytic efficiency are (i) the presence of electron-hole pairs on the surface, (ii) longer electron-hole recombination lifetimes, (iii) geometries providing higher surface-to-volume ratios, and (iv) a predominance of the anatase crystalline phase. Items (i)–(iii) are directly related to the material architecture.²⁷ With reference to the titania nanotubes¹⁹ considered herein, which are initially amorphous, crystallinity (iv) can be controlled through subsequent annealing of the initially amorphous nanotubes. In earlier work, we reported the ability to crystallize amorphous titania nanotubes with a high-temperature anneal;²⁸ both anatase and rutile phase are present after a 6 h, 500 °C anneal in oxygen. The anatase phase is optimal for photocatalytic

properties,²⁹ while the rutile phase provides titania with its hydrogen-sensing capabilities. After crystallization, the TiO₂ nanotube film was sputter-coated with a thin, discontinuous palladium layer; the palladium layer promotes catalytic dissociation of hydrogen molecules,³⁰ the ions of which are then adsorbed on the surface of the TiO₂ nanotubes.

At room temperature, approximately 24 °C, our hydrogen sensors, composed of a TiO₂-nanotube array with a 10-nm discontinuous Pd layer evaporated on the surface, demonstrate over a three orders of magnitude change in electrical resistance in response to 1000 ppm hydrogen. Furthermore, their photocatalytic properties are such that the hydrogen-sensing capabilities of the sensors are largely recovered by ultraviolet (UV) light exposure after being completely extinguished by the rather extreme means of sensor contamination: immersion of the sensor in motor oil.

II. EXPERIMENTAL

Titania-nanotube-array sensors were prepared by anodizing a titanium sheet (purity 99.9%, Sigma Aldrich) in a 1:7 acetic acid and 0.5% hydrogen fluoride electrolyte solution. The addition of acetic acid to the predominately HF solution results in more mechanically robust samples without changing the shape or size of the resulting nanotubes. A platinum counter-electrode was used. For our current study, we used an anodization voltage of 10 V resulting in nanotubes having an inner pore diameter of 22 nm and wall thickness of about 13.5 nm. The as-prepared amorphous titania nanotubes were then annealed at 500 °C for 6 h in oxygen resulting in crystallized titania having both anatase and rutile phases.²⁸ The samples were then coated with a 10-nm palladium layer by resistive evaporation. Field-emission scanning electron microscopy (FE-SEM) images revealed the Pd layer was deposited in the form of discontinuous nano-sized clusters.

The sensor measurement geometry is shown in Fig. 2. The sensors have one electrical contact on their surface,

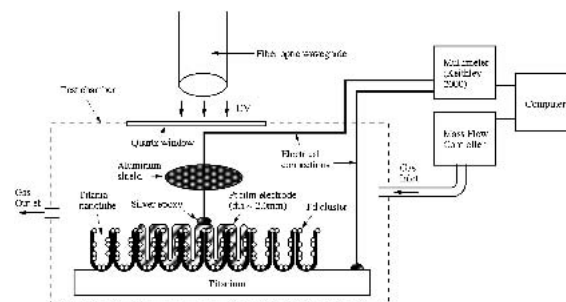


FIG. 2. Schematic diagram of experimental geometry used for investigating the self-cleaning capability of the titania-based room-temperature hydrogen gas sensor.

an rf-sputtered platinum pad approximately 2.0 mm in diameter, and an electrical contact to the underlying titanium foil. A 3.0-mm-diameter aluminum disk was placed approximately 3.0 mm directly above the platinum contact, shading it from the UV illumination to prevent degradation of the electrical contact. Why and how the UV degraded the electrical contact to the sensor, requiring the use of the aluminum disk to shade the contact from UV exposure, remains an unanswered question. All measurements were done at room temperature, approximately 24 °C.

The self-cleaning sensor experiments were performed in a 60 cm³ Plexiglas test chamber, with an opening for introducing the motor oil onto the sensor surface, and a quartz window for passing the UV illumination onto the sensor surface. Different grades of motor oil, 20W-50, 20W-40, 5W-30, and 10W-40 were used as sensor contaminants representing a rather extreme challenge to the sensor. The contaminated sensors were uniformly illuminated by 365-nm UV light, directed from the source (Hoya Schott, Model- HLS 210U, 150-W mercury xenon lamp) to the sensor surface through the use of a fiber optic waveguide to eliminate the possibility of heating the sensor surface. The intensity of the 365-nm UV light measured at the sensor surface was 270 mW/cm². The electrical resistance of a sensor was measured using a computer-controlled multimeter. A mass flow controller was used to regulate the H₂ + N₂ gas mixture and compressed air flow through the test chamber. We make note that stearic acid and cigarette smoke were also examined as sensor contaminants, with the sensor able to self-clean from these challenges in a fashion similar to that seen for the motor oil contamination. However, we were not able to poison uniformly the sensor using aerosolized contaminants, whereas a drop of motor oil upon the sensor was predictably able to extinguish the hydrogen-sensing capabilities of the sensor on a repeatable basis.

Photocatalytic measurements were performed on clean and motor-oil-contaminated Pd-coated TiO₂ nanotube samples as well as on uncoated TiO₂ nanotube samples. The electrochemical tests performed were cyclic voltammograms taken between -1.0 and 2.5 V using a potentiostat/galvanostat (Model-283, Princeton Applied Research). The instrument was connected to a PC, and the instrument-user interface was via the PowerCV software (Princeton Applied Research). Potentials were recorded against a silver-silver chloride reference electrode (Bio-analytical Systems) in a three-electrode cell where a platinum wire was used as the counter-electrode. The voltage was varied linearly at a scan rate of 20 mV/s. These tests were performed for both electrodes in 1 N KOH solution, prepared using KOH pellets (Fisher-Scientific) and de-ionized water and in acetonitrile (EM Science). Cyclic voltammogram curves at each different condition were taken both in the dark and under

illumination of a 365-nm UV lamp (EFOS Lite). The approximate radiant flux reaching the electrode surface, as measured by a radiometer/photometer (Model IL1400A, International Light) was 170 mW/cm² at 365 nm. For the experiments under illumination, the lamp waveguide was placed perpendicular to the electrode surface, on the outer wall of the Pyrex glass electrochemical cell.

III. RESULTS AND DISCUSSION

Figure 3 shows the real-time electrical resistance of an illustrative hydrogen sensor operated at room temperature in response to different atmospheres, contamination, and UV light exposures. The self-cleaning response of approximately 50 of the described hydrogen sensors have been examined over a period of 6 months, with results similar to that shown in Fig. 3. After flushing the test chamber with compressed air at a flow rate of 1000 sccm, the sensor was then exposed to a hydrogen-nitrogen mixture of 1000 ppm hydrogen. After reaching the saturation resistance, the gas was switched back to air with the sensor returning to its original state [Fig. 3(a)]. Prior to sensor contamination [Fig. 3(a)], we see a change in sensor resistance with exposure to 1000 ppm hydrogen of approximately 175,000%. While in air [Fig. 3(b)], the sensor was then contaminated with an approximately 0.06-mm layer of 10W-30 (Penzoil) motor oil after which the sensor demonstrated virtually no change in electrical resistance with hydrogen exposure over a period of approximately 10 min [Fig. 3(b) at time ≈ 1600]. We make note that the described TiO₂ nanotube hydrogen sensors are able to measure accurately hydrogen concentrations in electrical transformer oil, an application useful for prediction of transformer failure,³¹ and that the solubility of hydrogen in oil is approximately 7% by volume. However, in actual practice we have found it challenging to achieve hydrogen levels in oil above a few tens of ppm although hydrogen was bubbled through oil for several hours. Hence, while hydrogen can diffuse into oil where it would then—at least conceptually—be measured, with the oil-contamination of the sensor held in a hydrogen environment we see but little change in sensor resistance from time = 1600 s to time = 2200 s.

The oil-contaminated region on the sensor [Fig. 3(b)] was uniformly illuminated with UV light in the presence of air. The recovery of the sensor's hydrogen-sensing capability after UV illumination of 1-h duration can be seen in Figs. 3(b) and 3(c), 8 h duration in Fig. 3(b), and 10 h duration in Figs. 3(c)–3(d). As seen from Fig. 3(d), at the end of the UV-driven sensor-cleaning period, the measured relative change in electrical resistance with exposure to 1000 ppm hydrogen is 100,000%. The clean and recovered sensor has similar resistance values with exposure to air; the recovered sensor has a 1000 ppm

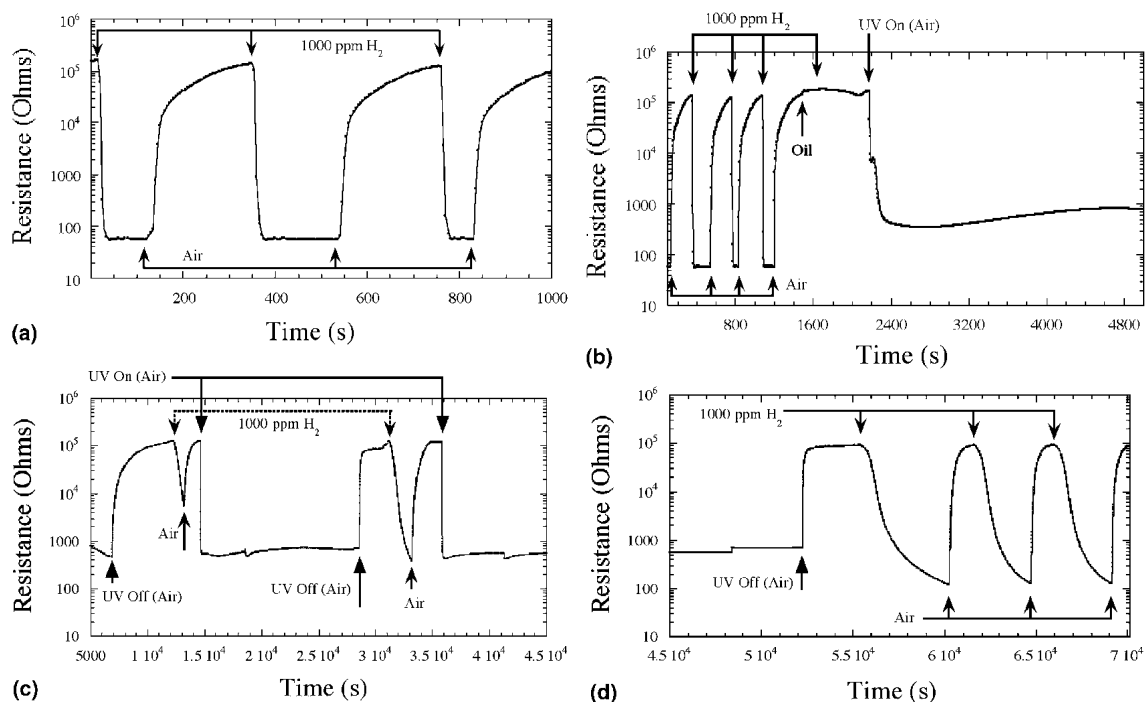


FIG. 3. A plot of real-time variation of resistance change before, during, and after cleaning the contaminant, motor oil 10W-30, with UV exposure. The plot, broken into four parts for clarity, shows (a) the original sensor behavior from time 10 s to 1000 s. (b) Behavior of sensor over time 100 s to 6000 s during which the sensor is contaminated with oil, losing its hydrogen-sensing capabilities, and is initially exposed to UV light. (c) The behavior of sensor from time 5000 s to 45,000 s. At time 7000 s, the UV is turned off, with the sensor regaining its nominal starting resistance of approximately 100,000 Ω , at which point it is exposed to 1000 ppm hydrogen and shows relative change in resistance of approximately 50. The sensor is then again exposed to UV, from roughly time 15,000 s to 29,000 s. After this second UV exposure, the sensor is again exposed to 1000 ppm hydrogen, showing an approximate factor of 500 change in electrical resistance. The sensor is once again exposed to UV, from time 36,000 s. (d) Sensor behavior from time 45,000 s to 70,000 s continues with UV exposure of the sensor to time 52,000 s, after which the sensor is repeatedly cycled between air and 1000 ppm hydrogen showing a relative change in impedance of approximately 1000. Compared to the hydrogen sensitivity of a noncontaminated sensor, the relative response of the “recovered” sensor is within a factor of two.

hydrogen resistance value of approximately 100 Ω compared to the 60 Ω value of the sensor prior to contamination.

We make note that the electrical resistance of the sensor rapidly drops with UV illumination due to photogeneration of charge carriers, yet after the UV light source is turned off, a relatively long time is required for resistance to be regained. The light source has a shutter that closes when the light source is turned off, and charge carrier lifetimes do not run into the minutes, so another mechanism underlies the relatively slow recovery in electrical resistance when the UV illumination ends. We suggest that adsorbed oxygen plays a major role in manipulating the conductivity. On UV illumination, the chemisorbed oxygen must be desorbed, increasing the conductivity. Hence, the conductivity increase with UV exposure has one part from the photogenerated current and another part from the electrons donated by the desorbed oxygen. On removing the UV illumination, oxygen will be re-adsorbed and hence the electrons will be extracted from the sensor. However, the process of oxygen re-adsorption is slow, on the order of several minutes, hence it takes a relatively long time to regain the original sensor resistance after the UV illumination is removed.

Multiple experiments were performed using 20W-40, 10W-40, and 5W-30 grade motor oils as sensor contaminants. The approximate thickness of the oil layer required to extinguish completely the sensor response to hydrogen was found to be approximately 0.03, 0.06, and 0.09 mm, respectively, corresponding to oil grades 20W-40, 10W-40, and 5W-30. The stepwise recovery of the sensors contaminated with different oil grades is shown by plotting relative resistance change ($R_{\text{air}}/R_{\text{H}}$) versus UV exposure duration in Fig. 4; the data points represent the average of three different sensors contaminated with the same grade oil. Here, R_{air} is the resistance of the clean sensor in air, generally equivalent to that of the contaminated sensor in air, and R_{H} is the steady-state resistance of the sensor exposed to 1000 ppm hydrogen. The value $R_{\text{air}}/R_{\text{H}}$ of the clean sensor is displayed at time equal -1 h, that of the contaminated sensor is shown at time equal zero. The plot clearly demonstrates the successive recovery of the $R_{\text{air}}/R_{\text{H}}$ value toward that of the clean sensor with incremental UV exposure. We make note that sensor poisoning by the lower-weight oil, 5W-30, requires a longer exposure duration to achieve recovery, possibly due to the relatively thicker film required to

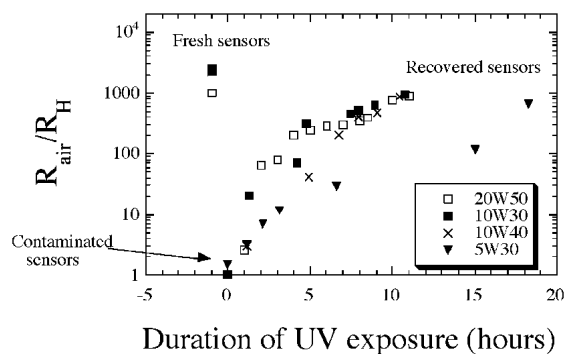
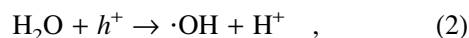
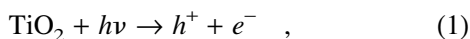


FIG. 4. A semi-log plot showing the stepwise improvement in sensor response with UV illumination of sensors contaminated with 20W-40, 10W-30, 10W-40, and 5W-30 motor oils. Here, the relative change in resistance of a sensor is measured with respect to 1000 ppm hydrogen as a function of duration of UV exposure. The fresh sensor is shown at arbitrary time while the dirty sensor is at zero hour. The data points represent the average response of five different sensors exposed to each contaminate (grade of motor oil).

contaminate the sensor. We found that the gas-sensing properties of sensors poisoned by a commercially available light-weight spray oil, WD-40 (San Diego, CA), could not be recovered with UV exposure. It is possible the WD-40 spray-oil contained products, such as phosphorous or sulfur, that formed oxidation products that in turn deactivated the oxidation capabilities of TiO₂.³²

It is well established that the presence of oxygen and water play a crucial role in the photocatalytic cleaning of titania²³ hence the sensor was exposed to air during UV exposure to facilitate removal of the oil from the sensor surface. In fact, it should be noted that UV exposure with the sensor kept in a nitrogen atmosphere did not result in sensor recovery. If the relevant redox potential of the contaminant does not lie within the bandgap of titania, the organic contaminants cannot be oxidized by photo-generated electron-hole pairs on the surface of titania. However, because the potential of water and oxygen exist within the bandgap of titania, the photogenerated holes in the valence band can oxidize water to produce highly reactive hydroxyl radical ($\cdot\text{OH}$), and the photo-generated electrons in the conduction band can reduce oxygen to form highly reactive superoxide ($\text{O}_2^{\cdot-}$) ions [Eqs. (1)–(3)], which then assist in oxidizing the organic species.



The overall quantum efficiency for steady-state photolysis depends on the interfacial charge transfer determined in the competition between charge carrier recombination and interfacial charge transfer. An increase in either the charge carrier recombination lifetime or the

interfacial electron transfer rate is expected to result in higher quantum efficiencies of the photodegradation reactions. Earlier work³³ has shown that Pd clusters on titania facilitates separation of photogenerated charge carriers, thereby increasing their recombination lifetime, and increases the rate of electron transfer to oxygen.^{33–35} In a size-quantized semiconductor system, Wang and co-workers³⁶ reported an increase in photocatalytic activity with a decrease in titania particle-size from 21 nm to 11 nm; however, the photocatalytic activity decreased when the size was further reduced to 6 nm. The results indicate that, depending on the nanoarchitecture, there exists an optimal particle size in nanocrystalline TiO₂ for maximum photocatalytic activity. Zhang and coworkers³⁷ explained these observations by correlating an increase in rate of interfacial charge carrier transfer with decrease in particle size; on reaching a certain limiting particle size, surface recombination exceeds the interfacial charge transfer process and therefore the photocatalytic activity reduced.

Figure 5 shows the cyclic voltammetry results for the clean Pd-coated titania nanotube sample in 1 N KOH electrolyte in both the dark and under UV illumination. Figure 6 shows the cyclic voltammetry results for the oil-contaminated Pd-coated titania nanotube sample in 1 N KOH electrolyte in both the dark and under UV illumination. The dark currents at positive potentials are low for both the clean and contaminated electrodes (Figs. 5 and 6), with some oxidation reaction related features³⁸ appearing at higher voltages. A possible reaction mechanism is³⁹:

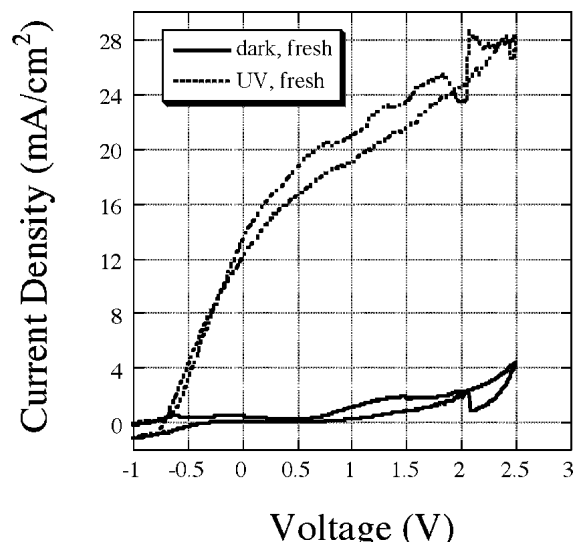


FIG. 5. Cyclic voltammograms for the clean Pd-coated titania electrodes measured in a 1 N KOH electrolyte in the dark and under UV illumination.

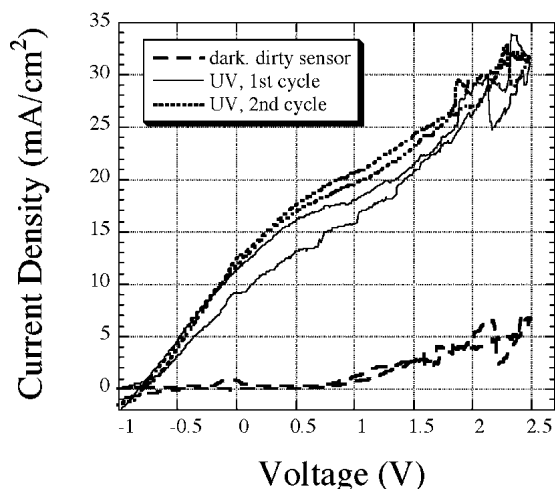


FIG. 6. Cyclic voltammograms for the oil-contaminated Pd-coated titania electrodes measured in 1 N KOH electrolyte in the dark and under UV illumination. The first cyclic voltammogram was taken immediately after contamination. The electrodes were then UV-illuminated for 5 min, then the second cyclic voltammogram recorded.



After the dark experiments, a cyclic voltammogram was taken under illumination. Then the electrode was exposed for 5 min to UV light and a cyclic voltammogram was again taken under illumination. This cycle was repeated for the clean and the contaminated electrodes. Upon illumination, the drastic change in the behavior at positive potential is a result of the onset of photo-current, generated from oxidative processes that occur via hole capture.⁴⁰ The anodic current density at 0.5, 1.5, and 2.5 V respectively are 2384, 27.3, and 6.5 times higher than in the dark, showing the onset of photocurrent from water oxidation via hole capture [Eq. (2)]. The magnitude of the photocurrent density under illumination for these palladium-sensitized titania electrodes is almost the same as that for those without the Pd coating. However, the Pd-sensitized electrodes have approximately four times greater dark current at positive potentials than the uncoated titania electrodes, presumably due to the Pd serving as an oxidation catalyst.⁴¹ Repeating the cyclic voltammograms according to the cycling process described above did not change the curves for the clean electrode. When the same UV exposure/cyclic voltammogram recording cycles were applied to the contaminated electrodes, a slight improvement of the photo-oxidation current was observed as shown in Fig. 6. After one cycle, the cyclic voltammogram curve nearly matches that of the clean one.

Motor oil is essentially a high-boiling-point paraffinic material obtained from petroleum fractions. It is chemically inert and relatively resistant to oxidation; we may reasonably expect that it will not undergo oxidation at ambient temperature. Because of its nonpolar nature, it is

essentially insoluble in water. The paraffinic chemical structure further indicates that it will be essentially insoluble in the 1 N KOH electrolyte. Furthermore, motor oil is not readily degradable by the action of UV-light alone, hence it appears that the improved anodic currents for the contaminated electrode under UV illumination must be a result of an oxidative process that eliminates the motor oil from the electrode.

IV. CONCLUSIONS

We demonstrate the self-cleaning capabilities of a titania-nanotube-based room-temperature hydrogen gas sensor. The titania nanotubes are made through an anodization process¹⁹ and subsequently crystallized by a high-temperature anneal.²⁸ A 10-nm coating of Pd was evaporated onto the surface of the titania nanotube array film to enhance the hydrogen sensitivity of the sensor, which showed over a 170,000% change in electrical resistance with exposure to 1000 ppm hydrogen at 24 °C. Upon intentional poisoning of the sensor with different grades of motor oil, the hydrogen-sensing capabilities of the sensor was essentially extinguished. With UV illumination, the photocatalytic properties of the titania nanotubes are such that the contaminant, a covering film of motor oil applied to the sensor as a liquid, is removed upon UV illumination enabling the sensor to recover effectively its original hydrogen sensitivity. Cyclic voltammetry was used to examine the underlying mechanisms of the photo-assisted degradation of oil from the sensor surface. Our results show a dramatic increase in photocurrent density to ~30 mA/cm² for both the clean and the oil-contaminated electrodes with UV illumination.

ACKNOWLEDGMENTS

The authors would like to thank Ms. Maggie Paulose for the FE-SEM images of the titania nanotubes and the two anonymous reviewers whose comments helped improve the manuscript quality.

REFERENCES

1. O.K. Varghese, D. Gong, M. Paulose, K.G. Ong, E.C. Dickey, and C.A. Grimes, *Adv. Mater.* **15**, 624 (2003).
2. M.C. Carotta, M. Ferroni, D. Gnani, V. Guidi, M. Merli, G. Martinelli, M.C. Casale, and M. Notaro, *Sens. Actuators B* **58**, 310 (1999).
3. N. Savage, B. Chwieroth, A. Ginwalla, B.R. Patton, S.A. Akbar, and P.K. Datta, *Sens. Actuators B* **79**, 17 (2001).
4. V. Guidi, M.C. Carotta, M. Ferroni, G. Martinelli, L. Paglialonga, E. Comini, and G. Sberveglieri, *Sens. Actuators B* **57**, 197 (1999).
5. A. Ruiz, J. Arbiol, A. Cirera, A. Cornet, and J.R. Morante, *Mater. Sci. Eng. C* **19**, 105 (2002).
6. R.W. Matthews, *Water Research* **20**, 569 (1986).
7. A. Mills and S.L. Hunte, *J. Photochem. Photobio. A* **108**, 1 (1997).

8. I.K. Konstantinou and T.A. Albanis, *Appl. Catal. B* **42**, 319 (2003).
9. K. Tanaka and K.S.N. Reddy, *Appl. Catal. B* **39**, 305 (2002).
10. M.M. Higarashi and W.F. Jardim, *Catalysis Today* **76**, 201 (2002).
11. S. Malato, J. Blanco, C. Richter, P. Fernández, and M.I. Maldonado, *Solar Energy Materials and Solar Cells* **64**, 1 (2000).
12. S. Chiron, A. Fernandez-Alba, A. Rodriguez, and E. Garcia-Calvo, *Water Research* **34**, 366 (2000).
13. E. Vulliet, J-M. Chovelon, C. Guillard, and J-M. Herrmann, *J. Photochem. Photobio. A* **159**, 71 (2003).
14. J.C. Garcia and K. Takashima, *J. Photochem. Photobio. A* **155**, 215 (2003).
15. A. Vidal, Z. Dinya, F. Mogyorodi, Jr., and F. Mogyorodi, *Appl. Catal. B* **21**, 259 (1999).
16. E. Moctezuma, E. Leyva, E. Monreal, N. Villegas, and D. Infante, *Chemosphere* **39**, 511 (1999).
17. V. Maurino, C. Minero, E. Pelizzetti, and M. Vincenti, *Colloids Surf. A* **151**, 329 (1999).
18. E. Pelizzetti, V. Maurino, C. Minero, O. Zerbinati, and E. Borgarello, *Chemosphere* **18**, 1437 (1989).
19. D. Gong, C.A. Grimes, O.K. Varghese, W. Hu, R.S. Singh, Z. Chen, and E.C. Dickey, *J. Mater. Res.* **16**, 3331 (2001).
20. M.R. Hoffmann, S.T. Martin, W. Choi, and D.W. Bahnemann, *Chem. Rev.* **95**, 69 (1995).
21. R. Wang, K. Hashimoto, A. Fujishima, M. Chikuni, E. Kojima, A. Kitamura, M. Shimohigoshi, and T. Watanabe, *Nature* **388**, 431 (1997).
22. N. Sakai, A. Fujishima, T. Watanabe, and K. Hashimoto, *J. Phys. Chem. B* **107**, 1028 (2003).
23. P. Zeman and S. Takabayashi, *J. Vac. Sci. Technol. A* **20**, 388 (2002).
24. A. Mills and S-K. Lee, *J. Photochem. Photobiol. A* **152**, 233 (2002).
25. V. Rome, P. Pichat, C. Guillard, T. Chopin, and C. Lehaut, *New J. Chem.* **23**, 365 (1999).
26. D.X. Who, *J. Photochem. Photobiol.* **137**, 53 (2000).
27. D. Beydoun, R. Amal, G. Low, and S. McEvoy, *Journal of Nanoparticle Research* **1**, 439 (1999).
28. O.K. Varghese, M. Paulose, D. Gong, C.A. Grimes, and E.C. Dickey, *J. Mater. Res.* **18**, 156 (2003).
29. B. Ohtani, Y. Ogawa, and S. Nishimoto, *J. Phys. Chem. B* **101**, 3746 (1997).
30. M.A. Pick, J.W. Davenport, M. Strongin, and G.J. Dienes, *Phys. Rev. Lett.* **43**, 286 (1979).
31. J. Bodzenta, B. Burak, Z. Gacek, W.P. Jakubik, S. Kochowski, and M. Urbanczyk, *Sens. Actuators B* **87**, 82 (2002).
32. M. Abdullah, G.K-C. Low, and R.W. Matthews, *J. Phys. Chem.* **94**, 6820 (1990).
33. S. Zheng, L. Gao, Q. Zhang, and J. Sun, *J. Solid State Chem.* **162**, 138 (2001).
34. C-M. Wang, A. Heller, and H. Gerischer, *J. Am. Chem. Soc.* **114**, 5230 (1992).
35. J. Papp, H-S. Shen, R. Kershaw, K. Dwight, and A. Wold, *Chem. Mater.* **5**, 284 (1993).
36. C-C. Wang, Z. Zhang, and J.Y. Ying, *Nanostruct. Mater.* **9**, 583 (1997).
37. Z. Zhang, C-C. Wang, R. Zakaria, and J.Y. Ying, *J. Phys. Chem. B* **102**, 10871 (1998).
38. A. Hagfeldt and M. Graetzel, *Chem. Rev.* **95**, 49 (1995).
39. M.M. Jaksic, *International Journal of Hydrogen Energy* **26**, 559 (2001).
40. A. Zaban, A. Meier, and B.A. Gregg, *J. Phys. Chem. B* **101**, 7985 (1997).
41. L.N. Lewis, *Chem. Rev.* **93**, 2693 (1993).